LAWRENCE
LIVERMORE
NATIONAL
LABORATORY

UCRL-JRNL-211525

The Filamentary Large Scale Structure around the z=2.16 Radio Galaxy PKS 1138-262

S. Croft, J. Kurk, W. van Breugel, S. A. Stanford, W. de Vries, L. Pentericci, H. Rottgering

April 19, 2005

Astronomical Journal

DRAFT VERSION APRIL 13, 2005
Preprint typeset using LaTeX style emulateapj v. 2/19/04

THE FILAMENTARY LARGE SCALE STRUCTURE AROUND THE Z = 2.16 RADIO GALAXY PKS 1138-262

STEVE CROFT[1], JARON KURK[2], WIL VAN BREUGEL[1], S. A. STANFORD[1,3], WIM DE VRIES[1], LAURA PENTERICCI[4] AND HUUB RÖTTGERING[5]

Draft version April 13, 2005

ABSTRACT

PKS 1138-262 is a massive radio galaxy at $z = 2.16$ surrounded by overdensities of Lyα emitters, Hα emitters, EROs and X-ray emitters. Numerous lines of evidence exist that it is located in a forming cluster. We report on Keck spectroscopy of candidate members of this protocluster, including nine of the 18 X-ray sources detected by Pentericci et al. (2002) in this field. Two of these X-ray sources (not counting PKS 1138-262 itself) were previously confirmed to be members of the protocluster; we have discovered that an additional two (both AGN) are members of a filamentary structure, at least 3.5 Mpc in projection, aligned with the radio jet axis, the 150 kpc-sized emission-line halo, and the extended X-ray emission around the radio galaxy. Three of the nine X-ray sources observed are lower redshift AGN, and three are M-dwarf stars.

Subject headings: galaxies: active — galaxies: individual (PKS 1138-262)

1. INTRODUCTION

PKS 1138-262 is a massive forming radio galaxy at z = 2.156 (Pentericci et al. 1998), which is surrounded by overdensities of Lyα emitters (Pentericci et al. 2000), Hα emitters (Kurk et al. 2004b), EROs (Kurk et al. 2004a) and X-ray emitters (Pentericci et al. 2002), several of which are spectroscopically confirmed to be close to the radio galaxy redshift. These overdensities appear to be spatially aligned with each other, and with the radio axis of PKS 1138-262 (§ 5).

At least half a dozen high redshift radio galaxies, with $2 < z < 5.2$, are now known to be located in such overdense regions (protoclusters; Venemans et al. 2002). Candidate members of such protoclusters may be found using color selection, line emission in a narrow band targeted at the redshift of interest, or X-ray emission – as noted above, when applied to the field of PKS 1138-262, these methods all revealed overdensities. Protoclusters have also been found using Lyman Break techniques (e. g. , Steidel et al. 1998) and deep millimeter and sub-mm observations (e. g. Ivison et al. 2000; Smail et al. 2003), and confirmed with spectroscopic follow-up. Due to the atmospheric cutoff, $z \sim 2$ is the lowest redshift at which the Lyα selection technique will work using ground-based optical instruments, but the technique has been successfully used to detect clumps and filamentary large scale structure even at $z \sim 6$ (e. g. , Ouchi et al. 2005, and references therein).

Recent simulations suggest that the colors of massive galaxies in the local Universe can only be explained if AGN feedback quenches star formation in the host galaxy (Springel et al. 2005). The link between supermassive black hole and galaxy formation (Haehnelt & Kauffmann 2000) may depend critically on AGN feedback, via coupling of the mechanical power (via winds or jets) of AGN to the baryonic component of forming galaxies (Rawlings 2003). The mergers, galaxy harassment, and other process invoked in AGN triggering, are common in clusters, and become increasingly important as redshift increases (Moore et al. 1998). High redshift clusters are dynamic regions at the nodes of the Large Scale Structure, where huge amounts of gravitational energy involved in structure formation may be dissipated. In order to understand the link between AGN, starburst and ULIRG galaxies (e. g. Nagar et al. 2003), and the life-cycle of a typical AGN, the study of AGN in clusters and protoclusters is important. Studies of the AGN / galaxy populations, kinematics, and substructures in protoclusters provide insight into how galaxies, AGN and clusters of galaxies form and evolve.

PKS 1138-262 is one of the first, brightest, and lowest redshift radio galaxy protoclusters discovered using Lyα narrowband selection techniques. By studying PKS 1138-262, we examine an important link between protoclusters at higher redshift, and their more evolved, virialised counterparts seen at $z \sim 1$ (Ford et al. 2004), and can help constrain models of structure formation and cosmology. This, and the many X-ray emitters with unknown redshifts, motivated us to obtain further spectra of candidate members of this protocluster using slitmasks at Keck. The previous spectroscopically confirmed overdensities led us to suspect that even more of these targets, in addition to some of the candidate Lyα emitters which did not yet have redshifts, would turn out to be members of the protocluster. If a large fraction of the X-ray sources turned out to be at the cluster redshift, this would suggest that the AGN activity in this cluster is unusually high, and if a large fraction of the Lyα sources turn out to be protocluster members, this would tend to suggest that star formation is also enhanced.

We assume an $\Omega_m = 0.27, \Omega_\Lambda = 0.73, H_0 = 71$ km s^{-1} Mpc^{-1} cosmology (Spergel et al. 2003). In comparing with the analyses of Kurk et al. (2000) and Pentericci et al. (2000) note that these authors use an $\Omega_m = 1.0, \Omega_\Lambda = 0.0, H_0 = 50$ km s^{-1} Mpc^{-1} cosmology. However, due to a calculation error, the comoving volume in the cosmology of these papers should have been 2740 Mpc^3 rather than the 3830 Mpc^3 quoted in Pentericci et al. (2000). In considering the comoving volume in which the objects are located, note also that, as discussed by Kurk et al. (2004a), the latest Lyα-candidate catalog is based on a rereduction of the imaging data of Kurk et al. (2000). The area used for detection by Kurk et al. (2004a) was 38.90 arcmin^2 (not, in fact, 43.6 arcmin^2 as stated by those authors), 10%

[1] Institute of Geophysics and Planetary Physics, Lawrence Livermore National Laboratory L-413, 7000 East Avenue, Livermore, CA 94550
[2] INAF, Osservatorio Astrofi sico di Arcetri, Largo Enrico Fermi 5, 50125, Firenze, Italy
[3] Department of Physics, University of California at Davis, 1 Shields Avenue, Davis, CA 95616
[4] Dipartimento di Fisica, Università degli Studi Roma Tre, Italy
[5] Leiden Observatory, Niels Bohrweg 2, NL-2333 CA Leiden, The Netherlands

larger than the 35.4 arcmin^2 used by Kurk et al. (2000) and Pentericci et al. (2000).

In our ΛCDM cosmology (similar to the cosmology of Kurk et al. 2004a), the comoving area of the field used for target selection is 98 Mpc^2. This yields a comoving volume of 4249 Mpc^3 probed by the spectroscopic observations (in the redshift range of 2.139 – 2.170), fortuitously rather close to the 3830 Mpc^3 of Pentericci et al. (2000). Using the redshift range of 2.110 – 2.164 probed by the narrow-band imaging (Kurk et al. 2000) yields a comoving volume of 7405 Mpc^3. The conclusions of Kurk et al. (2004a) are essentially unchanged, i. e. , we can estimate the strength of the overdensity to be a factor 2 ± 1. The conclusions of Pentericci et al. (2002) are also unaffected by our analysis as here the comparison to other fields is made on the basis of an areal overdensity.

2. KECK OBSERVATIONS

Our observations were made on 2004 January 19 – 20, using the Low Resolution Imaging Spectrometer (LRIS; Oke et al. 1995) on Keck I, with the D680 dichroic and a slit width of 1.5″. On the blue side, a 400 line / mm grism, blazed at 3400 Å was employed, giving 1.09 Å / pixel and spectral resolution 8.1 Å. On the red side, a 400 line / mm grating, blazed at 8500 Å was used, giving 1.86 Å / pixel and spectral resolution 7.3 Å. This setup gives spectral coverage of $\sim 3150-9400$ Å, although this varies somewhat from slitlet to slitlet. Two slitmasks were observed for 9000 s each. Seeing was 0.8″ during both sets of observations.

Our primary targets were randomly selected from those X-ray emitters of Pentericci et al. (2002) and candidate Lyα emitters of Kurk et al. (2004a) which did not yet have spectroscopically confirmed redshifts. Kurk et al. (2004a) select LEG (Lyα-emitting galaxy) candidates on the basis of excess narrow versus broad band flux, from which they calculate a continuum subtracted narrow band flux, $F = F_{NB} - F_B$ (where F_{NB} is the flux measured in a narrow band filter with central wavelength 3814 Å and FWHM 65 Å, and F_B is the flux measured in Bessel *B*-band). They also calculate a corresponding rest frame equivalent width, EW_0 (assuming that the narrow band excess is due to Lyα emission at $z = 2.16$). Their values of F and EW_0 for our targets are shown in Table 1.

Our slitmasks were designed by attempting to maximise the number of primary targets per mask. Gaps were then filled with secondary targets: five objects confirmed as members of the protocluster by Pentericci et al. (2000). In total we observed 31 targets (Table 1). The slitmasks were designed with slitlets ranging in length from $\sim 15-60''$, in all cases adequate for good sky subtraction.

The data were reduced in the standard manner using BOGUS[6] in IRAF, and spectra extracted in a 1.3″-wide aperture.

3. PROPERTIES OF THE SPECTROSCOPIC TARGETS

Table 1 summarises the results for all of our spectroscopic targets. Four targets were undetected and three showed continuum but no clear emission lines. Five showed an obvious single emission line which we were unable to unambiguously identify; since continuum is seen blueward of the line in these cases it is likely to be [O II] 3727. Assuming this to be the case, we assign redshifts in Table 1 but mark these instances with a question mark. In total we obtained secure redshifts for nineteen new targets which we classify on the basis of the broadness of spectral lines; [O III] / Hβ, [O II] / [O III] and other relevant line ratios (where these could be measured) and / or X-ray characteristics, as discussed below. Spectral lines were fit with Gaussian profiles using SPLOT in IRAF. For L968 (X3), where broad and narrow components are present, deblending was performed by fitting with multiple Gaussians. Measured parameters for the emission lines in those objects believed to be members of the PKS 1138-262 protocluster are listed in Table 2. All lines discussed below are in emission unless otherwise noted.

L54 — Previously confirmed at $z = 2.143$ by Pentericci et al. (2000). We obtain $z = 2.145$. Our spectrum is shown in Fig. 4.

L522 — Previously confirmed at $z = 2.166$ by Pentericci et al. We obtain $z = 2.161$ (see Fig. 4). The Lyα emission is extended (Fig. 2) over 2.7″ (23 kpc) across the slit (PA = 82°), due to the Lyα halo which encompasses this object and the radio galaxy (Kurk 2003).

L675 — Previously confirmed at $z = 2.163$ by Pentericci et al. (we measure $z = 2.162$; see Fig. 4), and also detect N V 1240.

L778 (X16) — A new spectroscopic confirmation at $z = 2.149$, showing broad Lyα (rest-frame deconvolved FWHM 890 km s^{-1}), N V 1240, C IV 1549, He II 1640, C III] 1909, [C II] 2326 and Mg II 2798 (Fig. 4).

L891 — Listed as a $z = 2.147$ Lyα emitter by Pentericci et al., this object was observed in *both* of our masks, and shows continuum blueward of the supposed Lyα line at 3828 Å, as well as an emission line at 7176 Å. We were unable to identify a plausible combination of emission lines arising from a single object at any redshift which could give rise to this line combination. We note, however, that in the 2D spectra (Fig. 3), the "Lyα" appears offset slightly (around 0.7″) from the continuum emission. This may be a LEG at the cluster redshift (we measure $z = 2.148$), while the continuum and 7176 Å emission line are continuum and [O II] 3727 from a foreground object at $z = 0.925$ (which also shows some evidence of a continuum break in around the right place for Ca H + K).

L968 (X3) — Previously confirmed at 2.183 (with caution that Lyα appears self-absorbed). We obtain $z = 2.162$, and see only slight self-absorption blueward of Lyα (Fig. 4). This AGN shows broad and narrow Lyα, broad and narrow C IV 1549, and broad N V. The C IV emission was fit with two Gaussian components, and the broad and narrow Lyα and N V were fit with three Gaussian components.

X2, X11 & X17 — Hα through Hζ at $z = 0$ are seen, along with molecular absorption bands. Comparison with the spectroscopic standards of Kirkpatrick, Henry, & McCarthy (1991) shows these three objects to be M-dwarf stars.

X5 — Faint but significant Lyα emission (rest-frame deconvolved FWHM 400 km s^{-1}); a new spectroscopic confirmation at $z = 2.162$ (Fig. 4). This object is also listed as an ERO (ERO 226; $I-K = 5.0$) by Kurk et al. (2004a). Although it is difficult to say, based on only the observed Lyα line, whether this object is a starburst or AGN, the soft X-ray to optical flux ratio (Pentericci et al. 2002), in addition to an inferred soft X-ray luminosity (4×10^{43} erg s^{-1}) much too high for a starburst, provide strong evidence for the presence of an AGN.

[6] http://astron.berkeley.edu/∼dan/homepage/bogus.html

X18 — This $z = 0.436$ Seyfert 2 shows strong [O II] 3727, [O III] 4959, 5007, [Ne III] 3869, [Ne V] 3426 and Hα lines. It is the nucleus of a galaxy undergoing a merger as seen on the VLT image.

4. DISCUSSION

All of the nine X-ray selected targets were spectroscopically detected and classified. Six of these were AGN, three of which are members of the protocluster $z \sim 2.2$ (including one reconfirmation). Two of these were also LEG candidates, showing again the efficacy of the narrow-band imaging selection method. Of the three lower-redshift AGN, one is at $z = 1.117$ (a member of the $z = 1.16$ spike discussed below).

The three remaining X-ray targets are M-dwarf stars. This is an unusually large fraction. Among the 42 objects with spectroscopic classifications in the Chandra Deep Field South catalog of Szokoly et al. (2004) only one X-ray source brighter than 10^{-15} erg s^{-1} cm^{-2} is an M-dwarf. So the X-ray overdensity in the PKS 1138-262 field is at least in part due to an excess of M-dwarfs in the foreground. However, with five out of 18 X-ray sources (including PKS 1138-262) now confirmed to be AGN this still suggests a higher AGN fraction in the PKS 1138-262 protocluster than in local clusters (see Pentericci et al. 2002) and in the fields of other HzRGs (Overzier et al. 2005).

Of the 24 targets selected on the basis of their Lyα excess, five were at the redshift of the protocluster (including four previously confirmed), seven were undetected or showed only faint continuum, and the remainder are most likely foreground galaxies. Four of these show a single emission line in the range 7927 – 8235 Å, which, if interpreted as [O II] 3727, places them at $z = 1.16 \pm 0.05$. The remaining five are at $z < 1$. The apparent overdensity at $z = 1.16$, which also includes L479 and X4 in addition to the four single-emission-line objects, makes it all the more necessary to obtain high quality spectra of targets in this field to determine whether they belong to this lower redshift system, or the PKS 1138-262 protocluster at $z = 2.2$. For example, the starburst galaxy L479 at $z = 1.171$ lies at the center of a $20''$-long string of six EROs (Kurk et al. 2004a), suggesting that at least some of the EROs may be physically associated with the $z = 1.16$ overdensity. Apparently, at this redshift, starburst galaxies with strong [O II] emission are also picked up by the Lyα selection process (at quite low significance) due to bluening of their continuum by young stars.

The pure LEG-selected targets in our multislit observations did not reveal additional PKS 1138-262 protocluster members (with the exception of L778, which is also an X-ray emitter). This is unlike the high success rate (up to 70%) of spectroscopically confirmed $z \sim 2.2$ LEGs reported by Pentericci et al. (2000). This is probably because objects with large *EW* (estimated from narrow-band photometry) are easiest to detect spectroscopically. However, these also tend to be the faintest objects in B-band (by definition) and large *EW combined with low expected Lyα flux* creates a signal-to-noise problem. Indeed, we see that our four non-detections are those listed by Kurk et al. (2004a) as having large *EW*, and comparatively low Lyα flux (Table 1).

To dispel any concern that our observations were less sensitive than those of Pentericci et al. (2000), note that the five of their confirmed $z \sim 2.2$ LEGs which we observed are reconfirmed by our observations (with the possible exception of L891, as noted above — which does in any case show a line which could plausibly be Lyα). In all cases except L968 (see discussion above), values of $1+z$ obtained are in agreement at the $\sim 0.2\%$ level. It seems therefore that our success rate in confirming Lyα emitters is lower simply due to our targets being those which are intrinsically fainter and / or closer to the cutoff of the selection criteria. We note that the Lyα selection technique has shown great success in other fields, particularly at higher redshift, and it is perhaps not surprising that our success rate is somewhat lower here due to redshifted Lyα being towards blue optical wavelengths. Here spectroscopic efficiency begins to drop, and the measurement of broad-band fluxes below the Lyα line or Lyman limit as an additional selection criterion is impossible due to the atmospheric cutoff.

5. CONCLUSIONS

There is still a good deal of evidence that PKS 1138-262 is located in a forming cluster; this conclusion is bolstered by our confirmation of two new objects at the same redshift as the radio galaxy. That one of these is also an ERO lends credence to the hypothesis that at least some of the ERO overdensity may be attributed to the protocluster. However, as noted by Steidel et al. (2000), the narrow-band (Equivalent Width) selection technique is effective but also difficult to quantify. Sensitive, wide spectral wavelength coverage is essential, the more so because there is a non-trivial chance that overdense fields at high redshifts maybe confused by other overdense fields in the foreground (van Haarlem, Frenk, & White 1997); another example of such a superposition of unrelated overdensities is seen by Francis et al. (2004). Curiously, Francis et al. also detect an object showing two emission lines which they are unable to indentify, similar to L891 as discussed above.

The confirmation that around one third of the X-ray sources in this field are associated with the protocluster ties in well with the conclusions of Pentericci et al. (2002) that there is a 50% excess of X-ray sources in the field of PKS 1138-262 compared to the Chandra Deep Fields. The high AGN fraction in PKS 1138-262 suggests that the AGN were probably triggered at around the same time, presumably by the ongoing formation of the protocluster. This supports models where AGN feedback is an important component of the early phases of galaxy and cluster formation. Intriguingly, our two new spectroscopic confirmations lie along the line of an apparent overdensity of spectroscopically-confirmed Lyα emitters (Fig. 1), in the same direction as the overdensity of X-ray emitters, radio axis of the central galaxy, extended X-ray emission around PKS 1138-262, and the general distribution of Hα emitters in the cluster (Pentericci et al. 2002). This is not entirely surprising if what we are seeing is a filament of the Large Scale Structure associated with this forming galaxy cluster.

The data presented herein were obtained at the W. M. Keck Observatory, which is operated as a scientific partnership among the California Institute of Technology, the University of California and the National Aeronautics and Space Administration. The Observatory was made possible by the generous financial support of the W. M. Keck Foundation. Work was performed under the auspices of the U. S. Department of Energy, National Nuclear Security Administration by the University of California, Lawrence Livermore National Laboratory under contract No. W-7405-Eng-48.

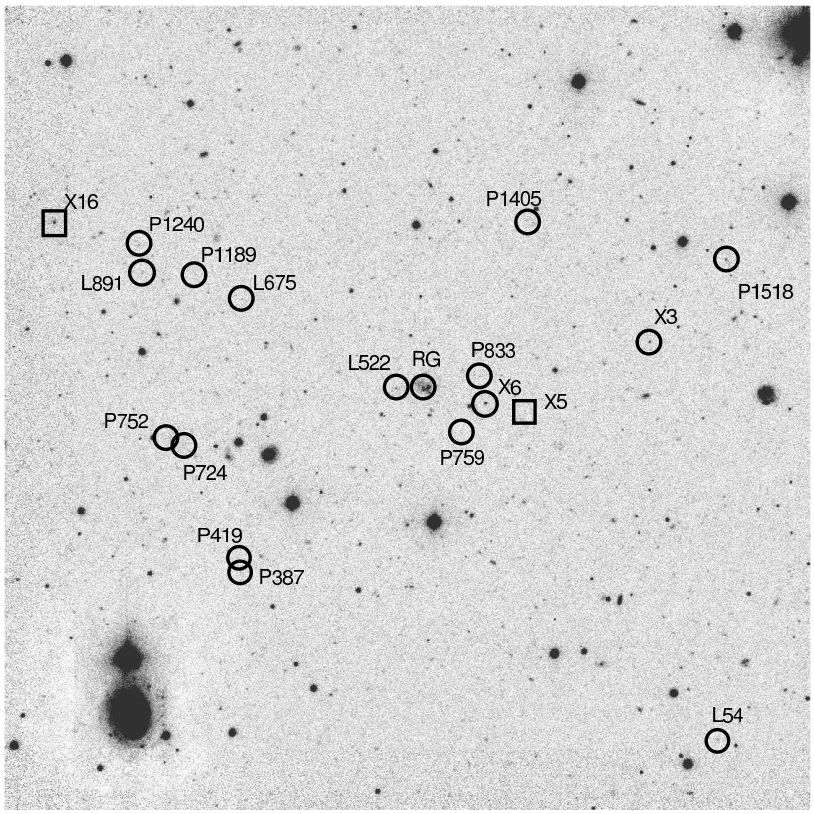

FIG. 1.—A 6.8′ × 6.8′ narrow-band (3814 Å) image of the field from VLT/FORS (Kurk et al. 2000). Previously confirmed protocluster members are indicated by circles (including L891, but see text). The 'L' and 'X' objects are labelled as in Table 1. Additionally the radio galaxy PKS 1138-262 is labelled 'RG', and the 'P' objects are labelled as in Pentericci et al. (2000). Note that the four 'L' objects, plus X3 (L968) are reobservations of targets from Pentericci et al. (2000); the two new confirmations from this paper are X5 and X16, and are indicated by squares.

REFERENCES

Best, P. N. 2000, MNRAS, 317, 720
Carilli, C. L., Harris, D. E., Pentericci, L., Rottergering, H. J. A., Miley, G. K., & Bremer, M. N. 1998, ApJ, 494, L143
Chambers, K. C., Miley, G. K., & van Breugel, W. 1987, Nature, 329, 604
Ford, H., et al. 2004, in Penetrating Bars through Masks of Cosmic Dust: The Hubble Tuning Fork Strikes a New Note, ed. D. L. Block, et al. (New York: Springer); astro-ph/0408165
Francis, P. J., Palunas, P., Teplitz, H. I., Williger, G. M., & Woodgate, B. E. 2004, ApJ, 614, 75
Haehnelt, M. G., & Kauffmann, G. 2000, MNRAS, 318, L35
Hill, G. J. & Lilly, S. J. 1991, ApJ, 367, 1
Ivison, R. J., Dunlop, J. S., Smail, I., Dey, A., Liu, M. C., & Graham, J. R. 2000, ApJ, 542, 27
Kirkpatrick, J. D., Henry, T. J., & McCarthy, D. W. 1991, ApJS, 77, 417
Kurk, J. D., et al. 2000, A&A, 358, L1
Kurk, J. D., Pentericci, L., Röttgering, H. J. A., & Miley, G. K. 2004, A&A, 428, 793
Kurk, J. D., Pentericci, L., Overzier, R. A., Röttgering, H. J. A., & Miley, G. K. 2004, A&A, 428, 817
Kurk, J. D. 2003, PhD Thesis, Leiden Observatory
Lacey, C. & Cole, S. 1993, MNRAS, 262, 627
Moore, B., Lake, G., & Katz, N. 1998, ApJ, 495, 139
Nagar, N. M., Wilson, A. S., Falcke, H., Veilleux, S., & Maiolino, R. 2003, A&A, 409, 115
Oke, J. B., et al. 1995, PASP, 107, 375
Ouchi, M., et al. 2005, ApJ, 620, L1
Overzier, R. A., Harris, D. E., Carilli, C. L., Pentericci, L., Röttgering, H. J. A., & Miley, G. K. 2005, A&A, 433, 87
Pentericci, L., Röttgering, H. J. A., Miley, G. K., Spinrad, H., McCarthy, P. J., van Breugel, W. J. M., & Macchetto, F. 1998, ApJ, 504, 139
Pentericci, L., et al. 2000, A&A, 361, L25
Pentericci, L., Kurk, J. D., Carilli, C. L., Harris, D. E., Miley, G. K., & Röttgering, H. J. A. 2002, A&A, 396, 109
Rawlings, S. 2003, New Astronomy Review, 47, 397
Simpson, C. & Rawlings, S. 2002, MNRAS, 334, 511
Smail, I., Scharf, C. A., Ivison, R. J., Stevens, J. A., Bower, R. G., & Dunlop, J. S. 2003, ApJ, 599, 86
Spergel, D. N., et al. 2003, ApJS, 148, 175
Springel, V., Di Matteo, T., & Hernquist, L. 2005, ApJ, 620, L79
Steidel, C. C., Adelberger, K. L., Dickinson, M., Giavalisco, M., Pettini, M., & Kellogg, M. 1998, ApJ, 492, 428
Steidel, C. C., Adelberger, K. L., Shapley, A. E., Pettini, M., Dickinson, M., & Giavalisco, M. 2000, ApJ, 532, 170
Szokoly, G. P., et al. 2004, ApJS, 155, 271
Venemans, B. P., et al. 2002, ApJ, 569, L11
van Haarlem, M. P., Frenk, C. S., & White, S. D. M. 1997, MNRAS, 287, 817

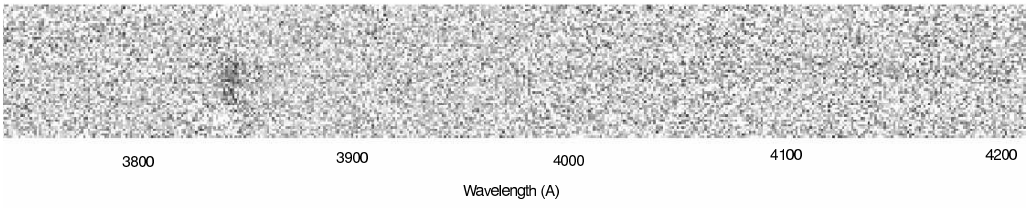

FIG. 2.—Two-dimensional spectrum of L522; the Lyα emission (observed wavelength 3844 Å) is spatially extended over a wider area than the continuum, showing the presence of the Lyα halo around this object.

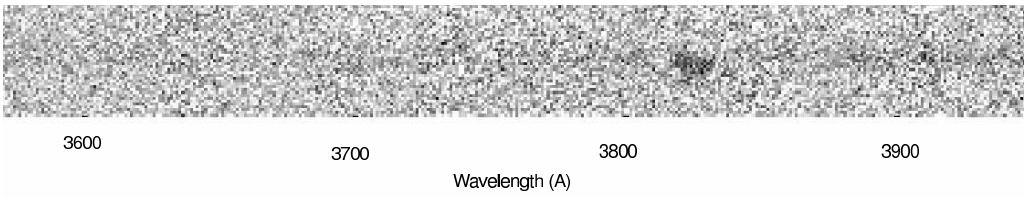

FIG. 3.—Two-dimensional spectrum of L891. The emission line at observed wavelength 3828 Å is most probably Lyα, but the continuum bluewards of this line casts doubt on this interpretation. The center of the line is offset by around 0.7″ from the continuum, suggesting that they may in fact be due to two separate objects.

TABLE 1
RESULTS OF SPECTROSCOPY FOR THE LEG CANDIDATE ('L') AND X-RAY ('X') SAMPLES.

ID [a]	RA	Dec	z	EW_0 [b]	F [c]	Notes
L46	11 40 33.89	–26 32 13.4	···	31.6	3.4	continuum
L54 [d, e]	11 40 37.15	–26 32 08.3	2.145	24.2	7.1	LEG P7
L73	11 40 37.75	–26 31 55.5	0.671	34.5	3.1	[O III] 4959, 5007; Hβ; starburst?
L127	11 40 48.21	–26 31 32.4	···	18.9	2.2	continuum
L184	11 40 36.63	–26 31 04.1	···	22.5	4.4	continuum
L286	11 40 47.92	–26 30 31.5	···	265.0	2.6	ND
L361	11 40 36.88	–26 30 08.8	0.913	23.6	4.3	[O II] 3727; [O III] 5007; broad Hγ; Hβ coincides with skyline; Seyfert 1?
L365	11 40 58.08	–26 30 09.4	1.127?	21.8	3.7	7927 Å emission line
L366	11 40 51.65	–26 30 08.0	0.861	29.5	5.0	Hβ; C III] 1909; strong [O II] 3727; AGN?
L470	11 40 59.71	–26 29 35.0	1.210?	49.9	3.9	8235 Å emission line
L479	11 40 51.05	–26 29 31.1	1.171	25.0	3.3	[O II] 3727; weak Hδ; starburst?
L484	11 40 45.52	–26 29 30.0	···	96.6	1.4	ND
L522 [d, e]	11 40 49.40	–26 29 09.6	2.161	36.0	20.0	LEG P856
L565	11 40 56.56	–26 26 13.6	0.496?	28.2	3.9	5574 Å emission line
L674	11 40 45.95	–26 28 35.7	···	269.4	2.6	ND
L675 [d, e]	11 40 55.29	–26 28 24.3	2.162	117.8	3.1	LEG P1612
L739	11 40 57.42	–26 27 07.8	1.125?	20.6	6.3	7919 Å emission line
L877	11 40 54.04	–26 28 01.1	0.863	31.6	4.3	[O II] 3727; narrow Hβ; weak H + K abs; starburst?
L891 [e]	11 40 59.07	–26 28 10.5	2.146?	25.4	4.7	P1557; see text
L941	11 40 44.04	–26 28 33.5	0.800	32.0	3.3	Hβ; [O III] 4959, 5007; starburst?
L942	11 40 49.84	–26 28 29.0	···	55.3	2.9	ND
L980	11 40 42.31	–26 28 51.3	1.171?	113.1	4.7	8093 Å emission line
X2	11 40 38.83	–26 29 10.3	0.000	···	···	M-dwarf
X3 ≡ L968 [d, e]	11 40 39.69	–26 28 44.9	2.162	26.6	9.8	AGN P1687
X4	11 40 44.21	–26 31 29.8	1.117	···	···	[Ne IV] 2424; [O II] 3727; [Ne III] 3869; AGN
X5 [d]	11 40 44.46	–26 29 20.6	2.162	···	···	ERO, AGN
X9	11 40 52.83	–26 29 11.2	1.512	···	···	C IV 1549; He II 1640; C III] 1909; Mg II 2798; BL AGN
X11	11 40 54.66	–26 29 28.1	0.000	···	···	M-dwarf
X16 ≡ L778 [d]	11 41 02.41	–26 27 45.1	2.149	314.2	67.6	AGN
X17	11 41 02.99	–26 27 34.1	0.000	···	···	M-dwarf
X18 [f]	11 41 03.93	–26 30 48.4	0.436	···	···	Seyfert 2

NOTE. —Objects which were undetected in spectroscopic observations are marked "ND". All listed lines were detected in emission. Right ascension and declination are given in hours, minutes, and seconds, and degrees, arcminutes, and arcseconds, respectively, for equinox J2000.

[a] Catalog number from Kurk et al. (2004a).

[b] Rest-frame equivalent width (in Å) estimated from the continuum-subtracted narrow-band observations of Kurk et al. (2004a).

[c] Continuum-subtracted narrow-band flux (in 10^{-17} erg s^{-1} cm^{-2}) measured by Kurk et al. (2004a).

[d] Confirmed cluster member. See Table 2 for properties of the observed emission lines.

[e] Listed as spectroscopically confirmed protocluster member by Pentericci et al. (2000). Note that we find that one of these objects (L891) may not in fact be at the cluster redshift. The catalog numbers in Pentericci et al. (2000) do not match those in Kurk et al. (2004a); where applicable the Pentericci et al. IDs ('P') are given in the Notes column.

[f] Hard X-ray source. All other X-ray sources in the table are soft (Pentericci et al. 2002).

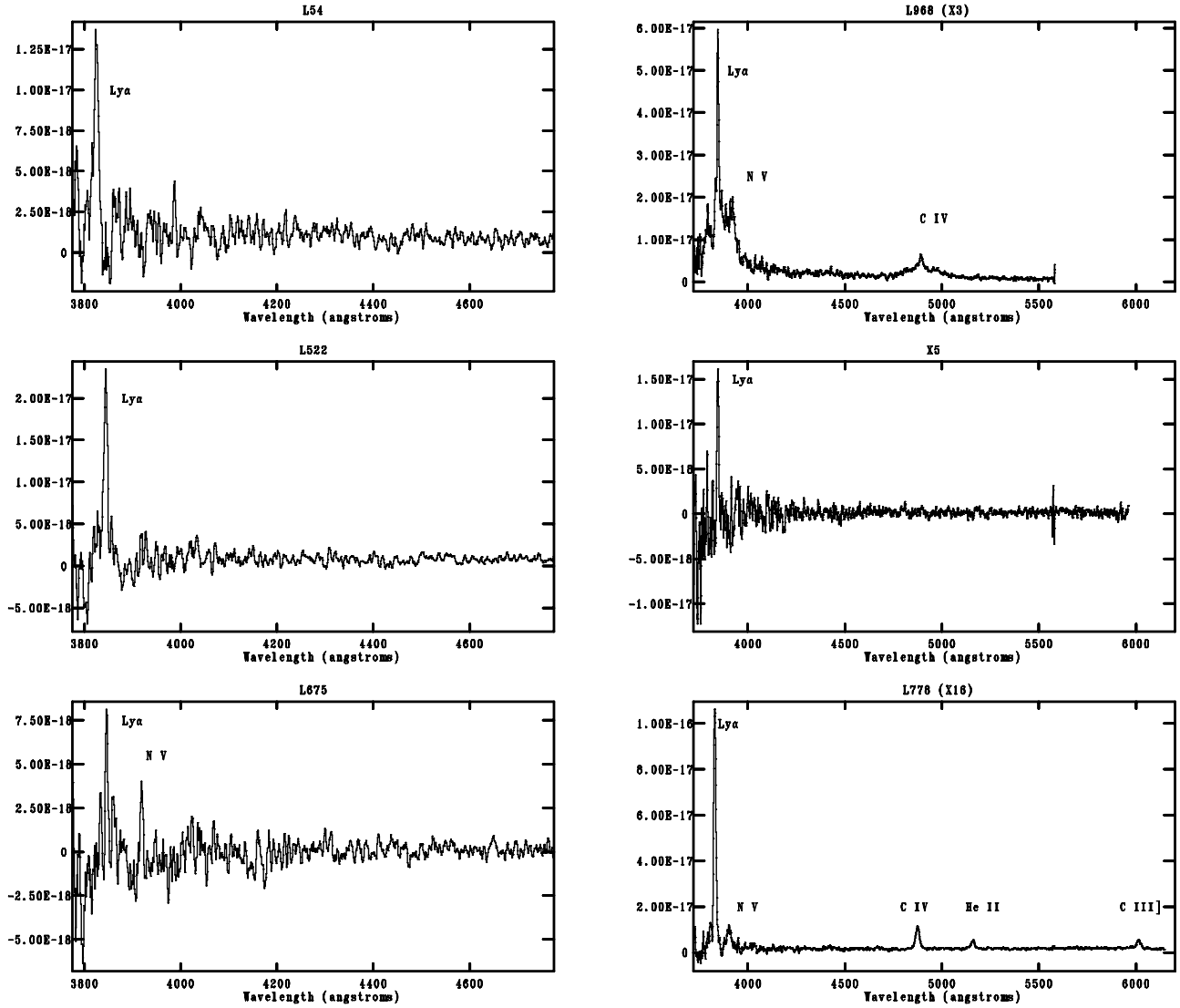

FIG. 4.—The LRIS-B (blue side) emission spectra of the objects from Table 1 confirmed to be in the $z \sim 2.16$ cluster, smoothed with a boxcar of width five pixels. Four of these objects were already spectroscopically confirmed by Pentericci et al. (2000); the two newly-confirmed $z \sim 2.16$ Lyα-emitters are X5 and L778 (X16). The X-ray emitters are shown plotted over a wider wavelength range, as unlike the LEG candidates, some show emission lines over this wider region. The y-axes show flux density in erg s^{-1} cm^{-2} Å^{-1}.

TABLE 2
PROPERTIES OF THE OBSERVED EMISSION LINES FOR PROTOCLUSTER MEMBERS.

ID	Line	λ_{rest} (Å)	λ_{obs} (Å)	FWHM (km s^{-1})	Flux (10^{-17} erg s^{-1} cm^{-2})	EW_0 (Å)
L54	Lyα	1216	3824	730 ± 20	15.7 ± 0.2	57.3 ± 0.6
L522	Lyα	1216	3844	230 ± 20	20.8 ± 0.1	57.0 ± 0.6
L675	Lyα	1216	3845	200 ± 30	6.4 ± 0.1	... [a]
	N V	1240	3919	200 ± 30	4.1 ± 0.1	... [a]
L891 [b]	Lyα $z = 2.148$?	1216?	3828	770 ± 20	23.9 ± 0.2	26.2 ± 0.2 [c]
	[O II] $z = 0.925$?	3727?	7176	220 ± 30	6.2 ± 0.2	49 ± 1 [c]
X3 $\equiv$ L968	Lyα broad	1216	3845	4790 ± 40	36.9 ± 0.2	157 ± 0.9
	Lyα narrow	1216	3845	122 ± 20	118.4 ± 0.8	49.0 ± 0.3
	N V	1240	3923	4041 ± 40	74.0 ± 0.6	89.8 ± 0.6
	C IV broad	1549	4895	12180 ± 280	48.2 ± 0.8	63 ± 2
	C IV narrow	1549	4884	1070 ± 50	5.7 ± 0.3	6.1 ± 0.3
X5	Lyα	1216	3845	400 ± 30	18.0 ± 0.1	... [a]
X16 $\equiv$ L778	Lyα	1216	3829	890 ± 20	158.4 ± 0.2	294.4 ± 0.4
	N V	1240	3901	2030 ± 20	24.0 ± 0.2	36.7 ± 0.3
	C IV	1549	4873	1430 ± 20	24.8 ± 0.2	54.5 ± 0.3
	He II	1640	5157	1360 ± 30	9.3 ± 0.2	19.3 ± 0.4
	C III]	1909	6012	1220 ± 40	10.0 ± 0.2	19.6 ± 0.4
	[C II]	2326	7334	1730 ± 210	4.0 ± 0.5	13 ± 2
	Mg II	2798	8822	960 ± 70	6.9 ± 0.4	11.5 ± 0.6

NOTE. —In contrast to Table 1, the values in this table are those measured from our Keck spectra.

[a] No continuum detected.
[b] Line identifications uncertain; this object may not be at the cluster redshift (see text).
[c] Assuming $z = 2.148$.